Magnetic properties of Fe$_5$SiB$_2$ and its alloys with P, S, and Co

Mirosław Werwiński[*]

Department of Physics and Astronomy, Uppsala University, Box 516, SE-751 20 Uppsala, Sweden
and Institute of Molecular Physics Polish Academy of Sciences, ul. M. Smoluchowskiego 17, 60-179 Poznań, Poland

Sofia Kontos, Klas Gunnarsson, and Peter Svedlindh

Department of Engineering Sciences, Uppsala University, Box 534, SE-751 21 Uppsala, Sweden

Johan Cedervall, Viktor Höglin, and Martin Sahlberg

Department of Chemistry, Uppsala University, Box 538, SE-751 21 Uppsala, Sweden

Alexander Edström, Olle Eriksson, and Ján Rusz

Department of Physics and Astronomy, Uppsala University, Box 516, SE-751 20 Uppsala, Sweden
(Received 2 March 2016; published 17 May 2016)

Fe$_5$SiB$_2$ has been synthesized and magnetic measurements have been carried out, revealing that $M_{sat} = 0.92$ MA/m at $T = 300$ K. The M versus T curve shows a broad peak around $T = 160$ K. The anisotropy constant K_1, estimated at $T = 300$ K, is 0.25 MJ/m^3. Theoretical analysis of Fe$_5$SiB$_2$ system has been carried out and extended to the full range of Fe$_5$Si$_{1-x}$P$_x$B$_2$, Fe$_5$P$_{1-x}$S$_x$B$_2$, and (Fe$_{1-x}$Co$_x$)$_5$SiB$_2$ compositions. The electronic band structures have been calculated using the full-potential local-orbital minimum-basis scheme (FPLO-14). The calculated total magnetic moments are 9.20, 9.15, 9.59, and 2.42 μ_B per formula units of Fe$_5$SiB$_2$, Fe$_5$PB$_2$, Fe$_5$SB$_2$, and Co$_5$SiB$_2$, respectively. In agreement with experiment, magnetocrystalline anisotropy energies (MAE's) calculated for $T = 0$ K change from a negative (easy-plane) anisotropy -0.28 MJ/m^3 for Fe$_5$SiB$_2$ to the positive (easy-axis) anisotropy 0.35 MJ/m^3 for Fe$_5$PB$_2$. Further increase of the number of p electrons in Fe$_5$P$_{1-x}$S$_x$B$_2$ leads to an increase of MAE up to 0.77 MJ/m^3 for the hypothetical Fe$_5$P$_{0.4}$S$_{0.6}$B$_2$ composition. Volume variation and fixed spin moment calculations (FSM) performed for Fe$_5$SiB$_2$ show an inverse relation between MAE and magnetic moment in the region down to about 15% reduction of the spin moment. The alloying of Fe$_5$SiB$_2$ with Co is proposed as a practical realization of magnetic moment reduction, which ought to increase MAE. MAE calculated in virtual crystal approximation (VCA) for a full range of (Fe$_{1-x}$Co$_x$)$_5$SiB$_2$ compositions reaches the maximum value of 1.16 MJ/m^3 at Co concentration $x = 0.3$, with the magnetic moment 7.75 μ_B per formula unit. Thus, (Fe$_{0.7}$Co$_{0.3}$)$_5$SiB$_2$ is suggested as a candidate for a rare-earth free permanent magnet. For the stoichiometric Co$_5$SiB$_2$ there is an easy-plane magnetization, with the value of MAE $= -0.15$ MJ/m^3.

I. INTRODUCTION

Volatile prices of the rare-earth elements observed in recent years have motivated wide research initiatives in an effort to find replacement materials for the permanent magnets industry, which would use little or none of the rare-earth elements. Late 3d transition elements, such as Mn, Fe, or Co are the primary candidates for such materials, thanks to their large and stable magnetic moments and high magnetic transition temperatures found in many of the compounds they form. However, weak spin-orbital interaction strength typically causes low magnetocrystalline anisotropy energy (MAE), which in turn means that they often lack appreciable coercivity, forming soft magnetic materials. Under certain circumstances, however, the MAE of 3d transition metal compounds can be substantial, for example, the tetragonally distorted Fe/Co alloys [1–5], L1$_0$ phases such as FeNi, CoNi, MnAl [6,7], Fe$_{16}$N$_2$ [8], (Fe/Co)$_2$B [9–12], or Fe$_2$P-based alloys [13,14]. A general overview on rare-earth-free permanent magnets is available in Ref. [15]. All of the above mentioned systems are hexagonal or tetragonal, i.e., uniaxial. For this reason, in this paper we have focused on an iron-based system Fe$_5$SiB$_2$ and its alloys

(Fe$_{1-x}$Co$_x$)$_5$SiB$_2$, Fe$_5$P$_{1-x}$S$_x$B$_2$, and Fe$_5$Si$_{1-x}$P$_x$B$_2$—they are tetragonal and rich on magnetic elements.

Fe$_5$SiB$_2$ [16] and Fe$_5$PB$_2$ [17] are isostructural with Cr$_5$B$_3$. They were initially reported by Aronsson and Engström [16] and Rundqvist [17] in 1960 and 1962. Several other borides crystallize within the same structure type. In the more general formula X_5SiB$_2$ for the silico-borides, X may stand for (Mn, Fe, Mo) [16], V [18], Nb [19] or W [20]. The recently discovered Nb$_5$SiB$_2$ and W$_5$SiB$_2$ have been recognized as superconductors. Isomorphous phases with phosphorus, X_5PB$_2$, were identified with $X =$ (Mn, Fe, Co) [17], Cr [21], and Mo [22].

The crystal structure of Fe$_5$PB$_2$ was determined by Rundqvist [17] and Fe$_5$SiB$_2$ by Aronsson and Engström [16], see Fig. 1. Rundqvist stated that the distribution of P and B atoms in Fe$_5$PB$_2$ was ordered and had a narrow homogeneity range [17]. Both Fe$_5$PB$_2$ and Fe$_5$SiB$_2$ crystallize in the Cr$_5$B$_3$-type structure [17] with body-centered tetragonal (bct) unit cell, space group $I4/mcm$, see Fig. 1(a). A single unit cell of Fe$_5$$XB_2$ contains 32 atoms divided into four formula units. Fe$_1$ atoms are distributed on the 16-fold position, B on the eightfold, Fe$_2$ and Si/P on the fourfold position.

The Fe$_5$SiB$_2$ and Fe$_5$PB$_2$ structures have a principally ordered arrangement of Si/P and B on their respective

———
[*]Corresponding author: werwinski@ifmpan.poznan.pl

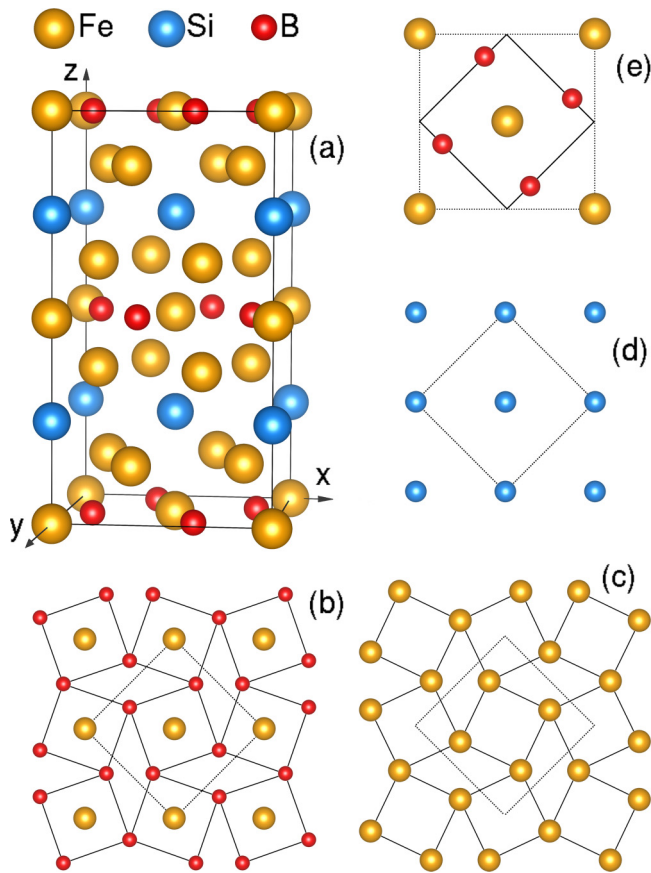FIG. 1. (a) The crystallographic structure of Fe_5SiB_2; (b) Fe_2-B layer; (c) Fe_1 layer; (d) Si layer; (e) Fe_2-B layer limited to the unit cell boundaries.

crystallographic sites, but some intermixing occurs as well as interstitial accommodations of B, Si, and P. Furthermore, octahedral holes of sufficient size for small nonmetal atoms exist in the system. Aronsson and Engström [16] found it likely that some of the boron atoms may be interstitially accommodated in these holes. Moreover, Rundqvist [17] described two types of holes in the Cr_5B_3-type lattice, trigonal prismatic and antiprismatic ones. In the Fe_5PB_2 system the radii of the trigonal prismatic and antiprismatic holes are 0.93 Å and 1.08 Å, respectively, while the B radius is 0.88 Å. A homogeneity range of Fe_5SiB_2 with the substitutions of B for Si has been observed previously. Fe_5SiB_2 measured by Aronsson and Engström [16] have B/Si ratio slightly larger than 2.00. The authors even proposed a new general formula, $Fe_5Si_{1-x}B_{2+x}$ ($0 < x < 0.1$). Another feature of Fe_5XB_2 structure is its layered character. The structure is built up of three types of layers, which alternate along the c axis. A single unit cell consists of 8 layers: 2 Fe-B, 4 Fe, and 2 Si layers, see Fig. 1.

At room temperature Fe_5SiB_2 and Fe_5PB_2 are ferromagnets with an orientation of spins parallel to the tetragonal axis [23]. The Curie temperature (T_C) is slightly varying with the deviation from the stoichiometry ($Fe_5X_{1-x}B_{2+x}$), $T_C = 628 \pm 11$ K for Fe_5PB_2 [24], and $T_C \sim 784$ K for Fe_5SiB_2 [23]. For Fe_5PB_2 the tetragonal easy axis of the magnetization direction is valid from 80 K up to T_C [23]. The low temperature Mössbauer study of Fe_5SiB_2 revealed a significant change of the spectral shape

in the temperature range from 130 to 150 K [23]. Ericsson *et al.* [23] concluded that below 140 K the spins were oriented in the *ab* plane or close to that. There were also indications that below 140 K the pure ferromagnetic coupling is partly destroyed [23]. In the temperature region from 140 K up to T_C the Fe_5SiB_2 was confirmed to be a ferromagnet with the spins parallel to the c axis [23]. Häggström *et al.* [24] referred that an average magnetic moment of Fe_5PB_2 was reported to be 1.73 μ_B per Fe atom. The individual moments calculated by Häggström *et al.* from the values of the magnetic hyperfine fields are 1.6 μ_B for Fe_1 and 2.2 μ_B for Fe_2.

To the best of our knowledge there is no literature data concerning Co_5SiB_2, but only its homologue Co_5PB_2 [17]. Very recently, Co- and Mn-doped Fe_5SiB_2 and Fe_5PB_2 were synthesized and characterized [25]. Another recent paper reports a study of a single crystal of Fe_5PB_2 [26]. Both these studies also report basic characterization of the electronic structure of the parent compounds, Fe_5SiB_2 and Fe_5PB_2, respectively.

II. EXPERIMENTAL AND COMPUTATIONAL DETAILS

A. Experimental details

Fe_5SiB_2 samples were prepared using a conventional arc furnace in an argon atmosphere. Stoichiometric amounts of iron (Leico Industries, purity 99.995%, surface oxides were reduced in H_2-gas), silicone (Highways International, purity 99.999%) and boron (Wacher-Chemie, purity 99.995%) were used as raw materials. The samples were crushed, pressed into pellets, and sealed in silica tubes, annealed at 1273 K for 19 days and then quenched in cold water.

X-ray powder diffraction intensities (XRD) were recorded using a Bruker D8 diffractometer with a Våntec position sensitive detector with a 4° opening using $CuK\alpha_1$ radiation, $\lambda = 1.540598$ Å. The measurements were taken in a 2θ range of 20–90°. Phase analysis and crystal structures refinements were performed using the Rietveld method [27] implemented in the software FullProf [28], and cell parameters were refined using the software UNITCELL [29].

Magnetization measurements on the powder samples were performed using a Quantum Design PPMS 6000 vibrating sample magnetometer. The low field magnetization temperature dependence was recorded between $T = 300$ K and $T = 10$ K at a constant magnetic field of 8 kA/m. The magnetization M versus field H at constant temperatures $T = 30$ K, 165 K, and 300 K, respectively, was measured in the range from -4 MA/m to $+4$ MA/m.

B. Computational details

Fully relativistic electronic band structure calculations were carried out by using the full-potential local-orbital minimum-basis scheme (FPLO-14.0-49) [30] within the generalized gradient approximation (GGA) for the exchange-correlation potential in the Perdew, Burke, Ernzerhof form (PBE) [31]. Calculations were performed with $16 \times 16 \times 16$ **k** mesh and convergence criterion 10^{-8} Ha. An initial spin splitting is applied to the $3d$ atoms, assuming ferromagnetic structures, as observed experimentally.

System	a [Å]	c [Å]	x_{Fe_1/Co_1}	z_{Fe_1/Co_1}	x_B
Fe_5SiB_2	5.546	10.341	0.169	0.136	0.382
Co_5SiB_2	5.511	9.953	0.169	0.134	0.376
Fe_5PB_2	5.503	10.347	0.172	0.138	0.383
Fe_5SB_2	5.466	10.594	0.172	0.138	0.383

For Fe_5SiB_2, Co_5SiB_2, Fe_5PB_2, and Fe_5SB_2 the lattice parameters and the internal atomic positions were optimized, see Table I. The optimized structural parameters of Fe_5SiB_2 and Fe_5PB_2 are in an excellent agreement with the corresponding experimental values [17,23]. We note that the computationally relaxed structural parameters reported here are for the stoichiometric phases of Fe_5SiB_2 and Fe_5PB_2, while the previously measured values are estimated from nonfully stoichiometric samples.

Virtual crystal approximation (VCA) is used to study three ranges of compositions, the first one between Fe_5SiB_2 and Co_5SiB_2, the second one between Fe_5SiB_2 and Fe_5PB_2, and the last one between Fe_5PB_2 and Fe_5SB_2. The general idea of the VCA is to imitate a homogeneous random on-site occupation of two types of atoms by using a virtual atom with a corresponding averaged value of the nuclear charge and number of electrons. Application of VCA for Fe/Co alloying is motivated by the fact that Co atomic number is one above Fe and furthermore that similar VCA calculations have already produced realiable results for other Fe/Co alloys [3,5,11]. Since P and Si are also neighbors in the periodic table, and as the p-elements are basically supplying itinerant electrons to the crystal, the VCA is expected to be a good approximation of the substitutional disorder also for this class of systems. The same argument holds for P/S alloying. It is important to comment that although VCA is expected to give the right qualitative trends of MAE changes with Fe/Co concentration, the exact values of MAE are usually overestimated by a factor between 2 and 4 in comparison to experiment. More accurate results of MAE can be calculated within the coherent potential approximation (CPA) [11,32–34]. Unfortunately, the utilized version of the FPLO code (v. 14.0-49), which allows to perform the spin-orbit coupling (SOC) calculations together with fixed spin moment (FSM), does not allow to combine SOC with CPA. Calculations for $Fe_5Si_{1-x}P_xB_2$ compositions start from the Fe_5SiB_2 structure with a full Si site occupation. The Si atom is then replaced by a virtual atom to mimic the specific composition. The atomic number of virtual atom is $Z_{VCA} = (1-x) \cdot Z_{Si} + x \cdot Z_P$. The lattice parameters of the intermediate compositions are interpolated linearly between the lattice parameters of the extreme systems. For every composition the internal atomic positions are optimized. The VCA calculations for $(Fe_{1-x}Co_x)_5SiB_2$ series are performed with lattice parameters and internal atomic positions interpolated as the linear combinations of crystal parameters of boundary compositions Fe_5SiB_2 and Co_5SiB_2. VESTA code [35] was used for visualization of crystal structures.
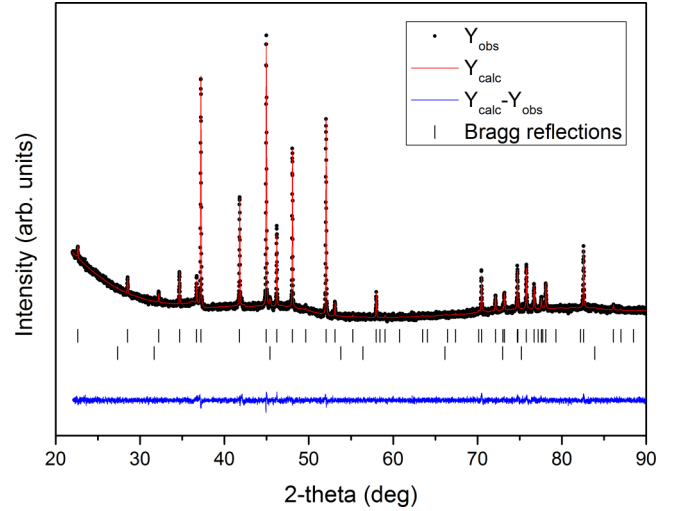

FIG. 2. X-ray powder diffraction pattern of Fe_5SiB_2 refined with the Rietveld method. The black dots and the red line correspond to the observed and calculated patterns, respectively, while the blue line shows the difference between observed and calculated data. Bars show the theoretical Bragg peaks of the Fe_5SiB_2 phase (upper) and the impurity phase, Fe_3Si (lower).

III. EXPERIMENTAL RESULTS

A. Phase analysis and crystal structure

The XRD intensities, presented in Fig. 2, confirm that Fe_5SiB_2 crystallizes in the tetragonal Cr_5B_3-type structure with the space group $I4/mcm$ [16]. Synthesized sample contains less than 2 at.% of an additional Fe_3Si impurity phase.

Table II presents the atomic coordinates of Fe_5SiB_2 structure derived from crystal structure refinement of XRD data. Determined lattice parameters are $a = 5.5561(3)$ Å and $c = 10.3476(10)$ Å, estimated standard deviations are in the parenthesis. Previously reported Fe_5SiB_2 lattice parameters obtained by Ericsson [23] are $a = 5.43$ Å and $c = 10.33$ Å, in close agreement with our results. The Fe_5PB_2 lattice parameters are $a = 5.482$ Å and $c = 10.332$ Å [17]. It indicates that there are only few promiles differences between the calculated and measured lattice parameters for Fe_5SiB_2 and Fe_5PB_2, compare with Table I.

B. Measured magnetic properties

The value of M_{sat} (M at $H = 4$ MA/m) at $T = 300$ K is 0.92 MA/m (6.3 μ_B/f.u.) [cf. Fig. 3(a)] which is considerably smaller than expected from Mössbauer measurements, 1.2 MA/m (8.2 μ_B/f.u.). However, the Mössbauer data was

TABLE II. Atomic coordinates for Fe_5SiB_2 derived from crystal structure refinement of XRD data.

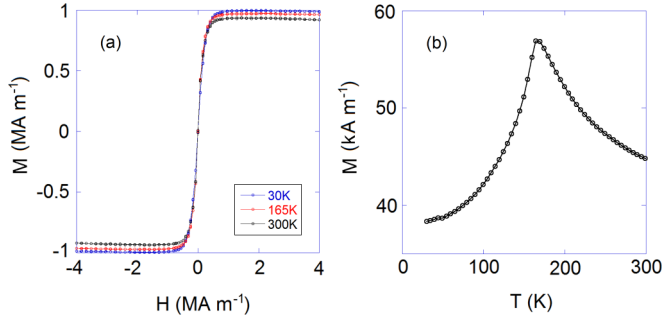| Atom	Site	x	y	z
Fe_1	16(l)	0.1683(1)	$\frac{1}{2} + x$	0.1384(1)
Fe_2	4(c)	0	0	0
Si	4(a)	0	0	$\frac{1}{4}$
B	8(h)	0.378(1)	$\frac{1}{2} + x$	0

FIG. 3. Results from magnetization measurements on Fe_5SiB_2. (a) Magnetization *versus* field at three different temperatures, top to bottom: $T = 30$ K, 165 K, and 300 K. (b) Magnetization *versus* temperature at a probing field of 8 kA/m.

reported for $T = 80$ K. Further, due to surface effects, M_{sat} for small particles should be lower than the bulk value. Also, there are nonmagnetic impurities in the sample, e.g., Fe_3Si, decreasing the estimated value of M_{sat}. Assuming the sample to consist of crystallites with uniaxial anisotropy, the anisotropy constant K_1 was estimated using the $1/H^2$ term in the law of approach to saturation. This term originates from competition between two energies; the field energy and the magnetocrystalline anisotropy energy:

$$\frac{M(H)}{M_{sat}} = \left(1 - \frac{a_2}{H^2}\right), \tag{1}$$

where

$$a_2 = \frac{4}{15}\left(\frac{K_1}{\mu_0 M_{sat}}\right)^2. \tag{2}$$

Using the *M versus H* measurement at $T = 300$ K [cf. Fig. 3(a)], the result for Fe_5SiB_2 is $K_1 = 0.25$ MJ/m³. Since Eq. (1) contains only the $1/H^2$ dependence of $M(H)$, the selection of field interval for the K_1 estimation is crucial. Here, the best fit was achieved using the field interval 0.6–1.0 MA/m, corresponding to $M(H)/M_{sat} = 0.95$–0.98. However, the need of a more accurate method, e.g., involving a single crystal sample, is emphasized and will be the aim for further experiments.

Concerning the proposed reorientation of spins at $T = 140$ K reported from Mössbauer experiments, the following observation was made from magnetization measurements: Referring to Fig. 3(b), the *M versus T* curve shows a broad peak around $T = 160$ K and then M decreases continuously with decreasing temperature, a maximum in *M versus T* signals the change of sign of K_1. Consequently, at the peak temperature, the value of K_1 must be close to zero and, hence, the system appears to be in a more magnetically soft state.

IV. DENSITY FUNCTIONAL THEORY CALCULATIONS

A. Fe_5SiB_2 electronic structure

The basic electronic configurations of the elements forming Fe_5SiB_2 are Fe: [Ar] $4s^2 3d^6$, Si: [Ne] $3s^2 3p^2$, and B: [He] $2s^2 2p^1$. This is reflected in the densities of electronic states (DOS), see Fig. 4. The total DOS is a sum of the individual atomic contributions, from which the dominant role is played by Fe $3d$ bands. Fe $3d$, Si $3s$, Si $3p$, B $2s$, and B $2p$
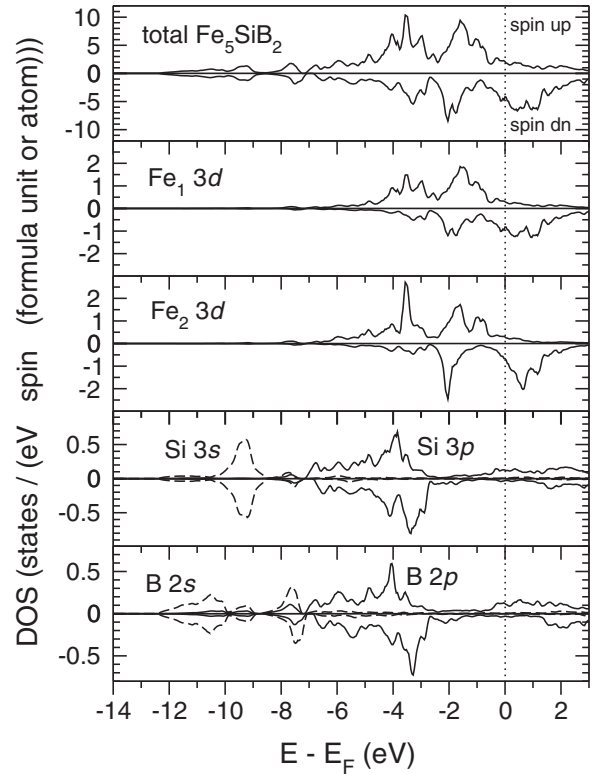

FIG. 4. The spin projected partial and total densities of states DOS for Fe_5SiB_2. Calculations done within GGA(PBE)+so approximation.

bands are presented on the spin projected DOS plots. The Fe bands Fe_1 $3d$ and Fe_2 $3d$, for two inequivalent Fe sites, are both strongly spin polarized. The corresponding spin magnetic moments are 1.87 and 2.24 μ_B/atom, respectively. The spin, orbital, and total magnetic moments are summarized in Table III. The Si and B spin magnetic moments are both equal to -0.25 μ_B.

From -2.5 eV up to the Fermi level the character of DOS originates almost entirely from Fe_1 $3d$ and Fe_2 $3d$ bands. It means that the main contribution to the DOS at the Fermi level is provided by the Fe $3d$ states, what moreover leads to high spin polarization on the Fermi level, of about 66%. Furthermore, calculations show that the orbital magnetic moments are present only on the Fe atoms (see Table III). Their values 0.039 μ_B and 0.048 μ_B are close to the value 0.043 μ_B

TABLE III. The spin, orbital, and total magnetic moments [μ_B/(atom or formula unit)] for Fe_5SiB_2, Co_5SiB_2, Fe_5PB_2, and Fe_5SB_2.

Atom	Fe_5SiB_2		Co_5SiB_2		Fe_5PB_2		Fe_5SB_2	
	μ_s	μ_l	μ_s	μ_l	μ_s	μ_l	μ_s	μ_l
Fe_1/Co_1	1.87	0.039	0.40	0.016	1.83	0.034	1.91	0.031
Fe_2/Co_2	2.24	0.048	0.90	0.025	2.22	0.052	2.26	0.048
Si/P/S	-0.25	0.001	-0.05	0.000	-0.14	0.003	-0.03	0.002
B	-0.25	0.001	-0.06	0.001	-0.22	0.001	-0.23	0.002
μ_{tot}	9.20		2.42		9.15		9.59	
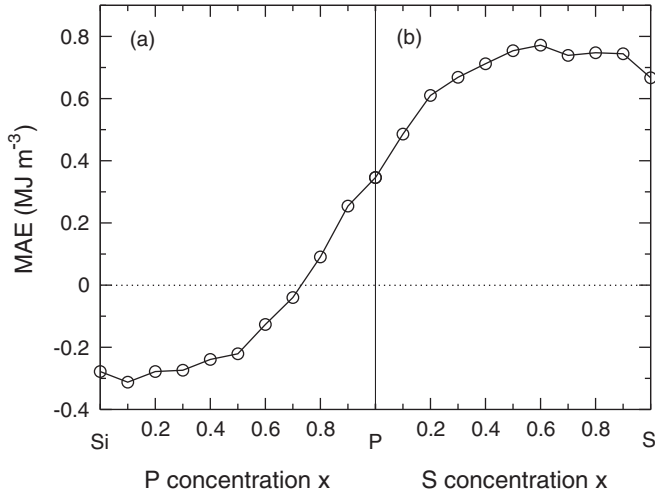
FIG. 5. The concentration dependency of the MAE for (a) $Fe_5Si_{1-x}P_xB_2$ and (b) $Fe_5P_{1-x}S_xB_2$.

for bcc iron, calculated within the same frame. Furthermore, the all theoretical values are reduced in comparison to the experimental value 0.086 μ_B for the bcc iron [36]. The total magnetic moment per formula unit is equal to 9.20 μ_B, which is in good agreement with the recently determined experimental value 9.35 μ_B/f.u. (5 × 1.87 μ_B/Fe) from $M(H)$ measurements at 10 K [37].

B. MAE of $Fe_5Si_{1-x}P_xB_2$ and $Fe_5P_{1-x}S_xB_2$

The Mössbauer study revealed the "in-plane" spin orientation for Fe_5SiB_2 below 140 K [23], in contrast to the "easy-axis" spin orientation for Fe_5PB_2 down to 80 K. As we are interested in materials with high magnetocrystalline anisotropy, we extend theoretical inquires of Fe_5SiB_2 by the promising uniaxial case of Fe_5PB_2. In this paper MAE is determined as the difference between total energies obtained for orthogonal spin quantization axes, MAE = $E_{100} - E_{001}$. Positive MAE value therefore denotes the uniaxial magnetocrystalline anisotropy along with easy axis 001 direction (tetragonal axis), whereas for negative MAE there is an easy-plane magnetization (*ab* plane). Calculated MAE of Fe_5SiB_2 and Fe_5PB_2 are −0.28 and 0.35 MJ/m³ (−140 and 170 μeV/f.u.), respectively. The negative and positive signs agree well with the experimentally observed magnetic structures [23]. For magnetic moment, going from Fe_5SiB_2 to

Fe_5PB_2, the most noticeable change is that of the induced spin magnetic moment on 3p element, from −0.25 to −0.14 μ_B (see Table III). The calculated total magnetic moments on Fe_1 and Fe_2 sites of Fe_5PB_2 are 1.86 and 2.27 μ_B/atom, respectively. They differ from experimental values 1.6 μ_B for Fe_1 and 2.2 μ_B for Fe_2, derived from the magnetic hyperfine fields [24], however the mentioned experimental values are only indirect approximate estimations.

A priori it is not obvious, what will be the evolution of MAE as a function of concentration x. As an example of nonmonotonic behavior we note the Fe/Co [1] or (Fe/Co)₂B alloys [10]. Therefore we have performed VCA studies of the $Fe_5Si_{1-x}P_xB_2$ for the whole range of compositions, $0 \leqslant x \leqslant 1$. The resulting VCA calculations of MAE versus x are presented in Fig. 5(a). The x dependence of MAE is monotonic except for the smallest values of P concentration. The MAE values for both stoichiometric concentrations are near extremal. With an increase of the P concentration the system is heading towards the uniaxial anisotropy, with a crossover at $x \gtrsim 0.7$. The transition from Si 3p^2 to P 3p^3 can be understood as an increase in the number of electrons in $Fe_5Si_{1-x}P_xB_2$ system. Further increase in the number of electrons can be realized by transition from P 3p^3 to S 3p^4. As shown in Fig. 5(b) for the hypothetical alloys with sulfur $Fe_5P_{1-x}S_xB_2$ significant values of MAE ~ 0.7 MJ/m³ are obtained for a broad range of sulfur concentration $0.4 \leqslant x \leqslant 1$.

In order to get deeper insight into the origin of MAE, the energy scale of the band structure has to be tenths of eV, since the SOC constant of 3d metals is in the order of 0.05 eV, which is also why the spin-orbit splitting does not exceed this value, see Fig. 6. Fully relativistic calculations result in an additional splitting of the electronic bands, due to spin-orbit coupling. The figure presents the Fe_5SiB_2 bands in the vicinity of the Fermi level, together with the MAE contributions per **k** point as obtained by the magnetic force theorem [38,39]. Spin-orbit splitting results in different band structures for quantization axes 100 and 001 indicated by red and blue lines.

The calculated total MAE of Fe_5SiB_2 is −140 μeV/f.u. (−0.28 MJ/m³). The MAE value $\sim 10^{-4}$ eV/f.u. indicates a fine compensation of the much bigger negative and positive contributions to MAE of about 10^{-3} eV per **k** point. Moreover, it is easy to notice the step changes of MAE(**k**) whenever the band crosses the Fermi level. Thus, when so many bands cross it, a very accurate model of the electronic band structure and fine **k** mesh are crucial to calculate MAE.
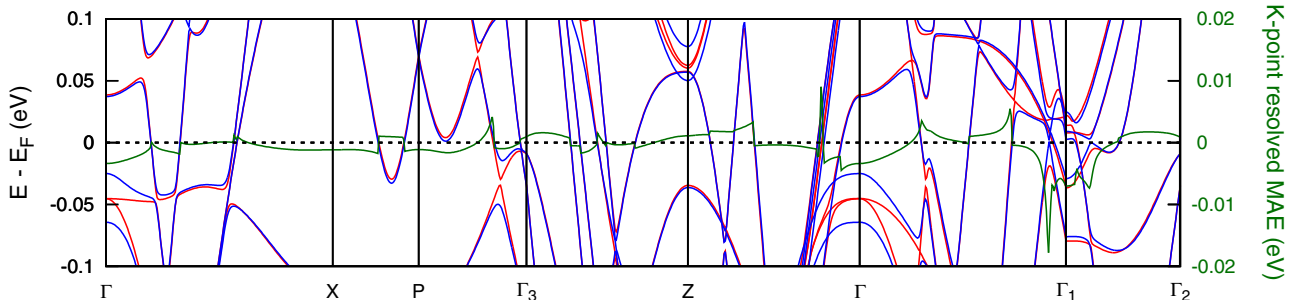

FIG. 6. Band structure of Fe_5SiB_2 calculated in fully relativistic approach for quantization axes 100 (red lines) and 001 (blue lines), together with the MAE contribution of each **k** point (green lines) as obtained by the magnetic force theorem.

C. Fe₅SiB₂ fixed spin moment and volume dependencies

For Fe₅SiB₂ the Mössbauer study revealed the "in-plane" spin orientation below 140 K and spins parallel to the c axis above 140 K [23]. A similar transition from negative to positive magnetocrystalline anisotropy constant was observed for Fe₂B with a transition temperature about 520 K [10]. Since the goal of this study is to explore for potential candidates for permanent magnets, the experimentally revealed increase of MAE with temperature for Fe₅SiB₂ has motivated theoretical studies which should allow for better understanding of this phenomena. To answer the question, whether the increase of MAE with T is related to the volume expansion, we have calculated volume dependency of MAE. Experimentally observed increase of volume between 16 and 165 K is about 0.01%, but for this small volume expansion no significant change of MAE is observed, see Fig 7. The performed calculations cover a much bigger range of volume change, namely from -10% to $+10\%$ and, what is striking, for a very large volume reduction the negative MAE change its sign, and for $V/V_0 = 0.9$ reaches significant value 0.52 MJ/m³. By a rough estimation, such volume reduction would correspond to about 20 GPa pressure, readily available in high pressure experiments [40].

Figure 8 shows nonlinear volume dependency of the total magnetic moment for Fe₅SiB₂. From Figs. 7 and 8 one could contemplate that MAE might increase when magnetic moment decreases. To address the question, whether the MAE changes in the same manner with only magnetic moment variation and without change of volume, a set of fully relativistic fixed spin moment (FSM) calculations was performed. Figure 9 presents the total magnetic moment ($M_S + M_L$) dependency of MAE. $M_S + M_L$ is evaluated for every fixed spin magnetic moment M_S.

FSM calculations show for Fe₅SiB₂ that MAE starts to increase with the decrease of total magnetic moment, and reaches the maximal value of MAE = 1.78 MJ/m³ for $M_S + M_L = 6.15$ μ_B/f.u., while equilibrium $M_S + M_L = 9.20$ μ_B/f.u. We suggest that significant increase of MAE might occur if we would find a way to reduce the magnetic moment of Fe₅SiB₂ by 1/3. A possible venue to achieve this could be alloying of magnetic element Fe with an
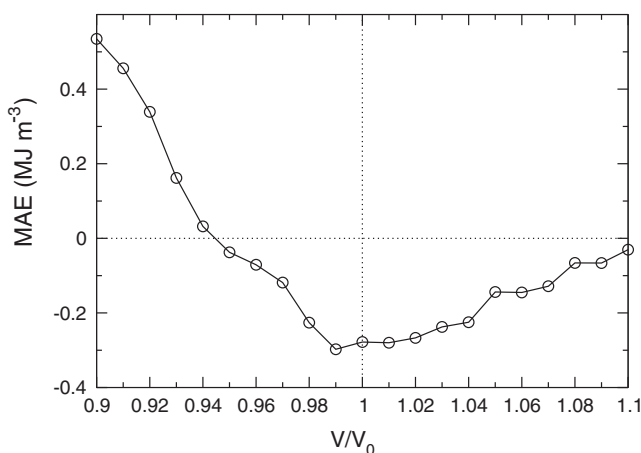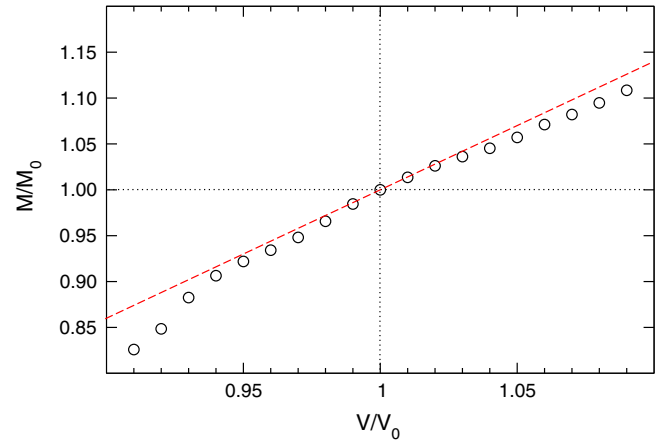

FIG. 8. The volume dependency of the magnetic moment for Fe₅SiB₂—black circles. For a better perception of its deviation from linearity the arbitrary (dashed) straight line is drawn.

element carrying a lower magnetic moment, Co. Following this idea the VCA calculations of $(Fe_{1-x}Co_x)_5SiB_2$ are carried out, expecting that alloying with Co will reduce magnetic moment, and hopefully in consequence increase the MAE. It is important to comment that reducing the magnetic moment by FSM or by alloying with another element will necessarily result in different changes to electronic structure, therefore we can't expect this analogy to hold, at least not up to large moment reduction. Nevertheless it is of interest to find out to what extent is this parallel realistic. Moreover, alloying of iron-based magnetic materials with Co has already been shown to lead to an increased MAE in several cases [1,3,4,11].

D. $(Fe_{1-x}Co_x)_5SiB_2$

VCA calculations of the whole range of $(Fe_{1-x}Co_x)_5SiB_2$ concentrations start from optimizing the extreme structures of Fe₅SiB₂ and Co₅SiB₂ (see Sec. II and Table I) and interpolating crystallographic parameters for intermediate compositions. The spin magnetic moments on Co₁ and Co₂ atoms in
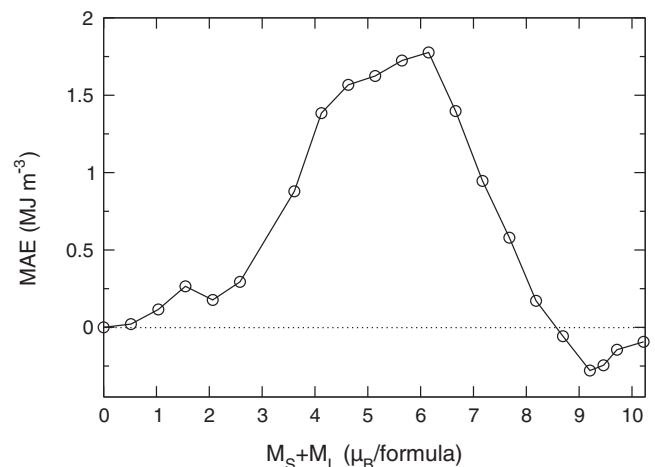

FIG. 9. The total magnetic moment dependency of the MAE for Fe₅SiB₂. Based on fully relativistic fixed spin moment (FSM) calculations.
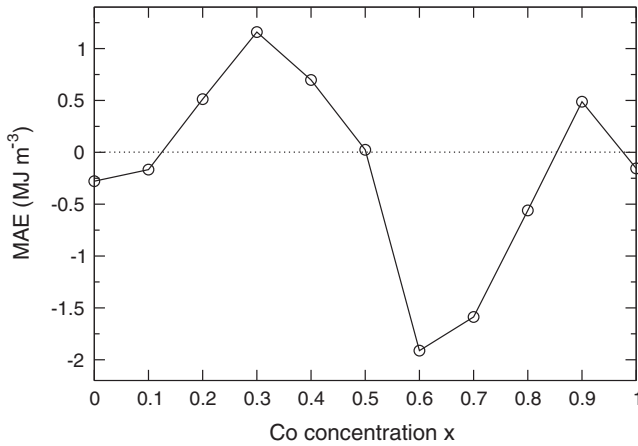

FIG. 7. The volume dependency of the MAE for Fe₅SiB₂.

FIG. 10. The Co concentration dependency of the MAE for $(Fe_{1-x}Co_x)_5SiB_2$.

Co$_5$SiB$_2$ are 0.41 and 0.90 μ_B, respectively. They induce the small opposite spin moments on Si and B, equal to -0.05 and -0.06 μ_B, respectively. The total magnetic moment per Co$_5$SiB$_2$ formula unit is equal to 2.42 μ_B (see Table III).

We expect that Fe/Co alloying will reduce the magnetic moment and thus may increase MAE of Fe$_5$SiB$_2$. The results of MAE(x) presented in Fig. 10 confirms our predictions partially. The maximum of MAE = 1.16 MJ/m^3 is obtained for $x = 0.3$ together with $M_S + M_L$ reduced from 9.20 to 7.75 μ_B/f.u., and not for 6.15 μ_B/f.u., as predicted for Fe$_5$SiB$_2$ from FSM. Figure 11 shows explicitly the dependence of MAE on $M_S + M_L$ for $(Fe_{1-x}Co_x)_5SiB_2$.

Our studies of MAE($M_S + M_L$) are then summarized in Fig. 12, where the total magnetic moment $M_S + M_L$ was varied by changing volume, fixed spin moment (FSM), or Fe/Co concentration. The MAE($M_S + M_L$) variations induced by FSM or volume scaling are very similar. The behavior of MAE($M_S + M_L$) related to alloying Fe$_5$SiB$_2$ with Co exhibit significant differences from the other two, which most probably roots in the change of the number of electrons in the system, accompanied with the Co alloying.

These differences can be examined based on the detailed band structure analysis as presented in Fig. 13. The energy
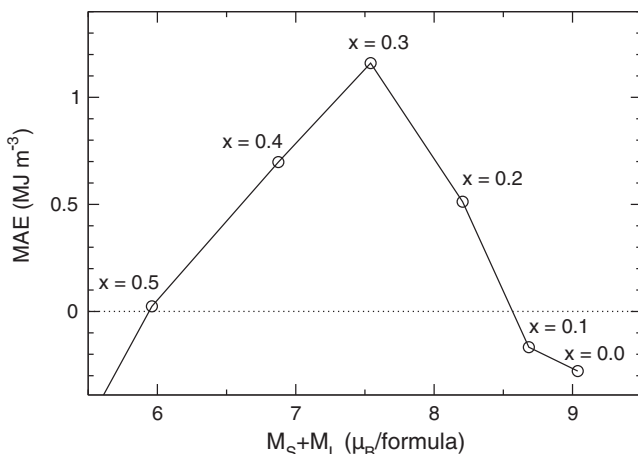

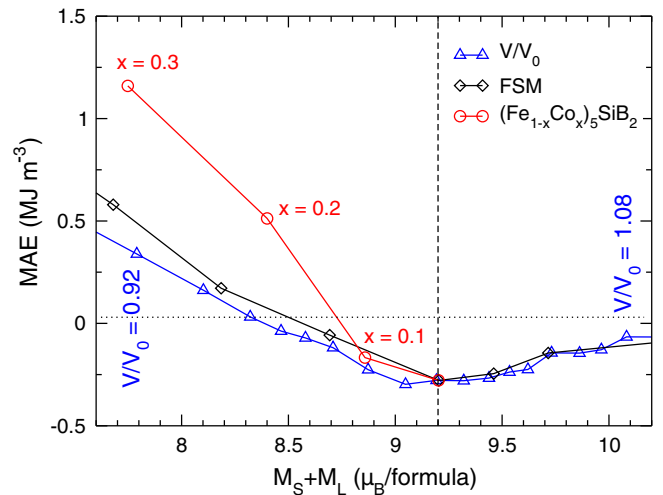FIG. 11. The total magnetic moment dependency of the MAE for $(Fe_{1-x}Co_x)_5SiB_2$.

FIG. 12. The total magnetic moment dependencies of the MAE for Fe$_5$SiB$_2$, mediated by volume variation (V/V_0), fixed spin moment (FSM), and alloying with Co $((Fe_{1-x}Co_x)_5SiB_2)$. Dashed line denotes equilibrium state with $x = 0$, $V/V_0 = 1$, and $M/M_0 = 1$.

window from -0.5 to 0.5 eV allows us to keep track of the variation of Fermi level with fixing spin moment FSM and doping with Co. Together with electronic bands the MAE contributions of each **k** point are presented as obtained by the magnetic force theorem [38,39]. The direction between high symmetry points X and P has been chosen because of the exceptionally simple form of bands in comparison to the other directions in Fig. 6. For X-P direction it is easy to notice how the band is filled with an increase of Co concentration x [panels (d), (e), (f), and (g)] or a corresponding behavior induced by reduction of spin moment [panels (d), (c), (b), and (a)]. The filling of the bands entails the change in MAE. In the energy window from -0.5 to 0.5 eV the differences in spin-orbit splitting for two quantization axes 100 and 001 might be difficult to notice. Nonetheless, the band structures calculated for two perpendicular quantization axes are marked in red and blue, respectively. Differences in spin-orbit splitting can be observed on several bands crossings. For Co concentration $x = 0$ [Fig. 13(d)] it is particularly easy to notice that the extra positive contribution to MAE is related to the band crossing Fermi level. For this band the 001 solution (blue line) lies slightly below the corresponding 100 band (red line), thus for the whole filled region, up to Fermi level, the positive contributions to MAE is observed.

The substantial differences in MAE($M_S + M_L$) mediated by FSM or Co alloying raise the question whether these two mechanisms work together. In Fig. 14 the FSM and VCA dependencies of MAE are presented in a form of two-dimensional color map in superposition with the theoretical equilibrium total magnetic moments ($M_S + M_L$). The MAE landscape reveals that by going from equilibrium magnetic moment of pure Fe$_5$SiB$_2$ towards the much lower equilibrium magnetic moment of Co$_5$SiB$_2$ the equilibrium MAE path (black dots) starts from negative sign, goes across the range of positive values, and follows through a steep hollow of negative values. This equilibrium path crossing the MAE landscape corresponds to the MAE (x) function presented
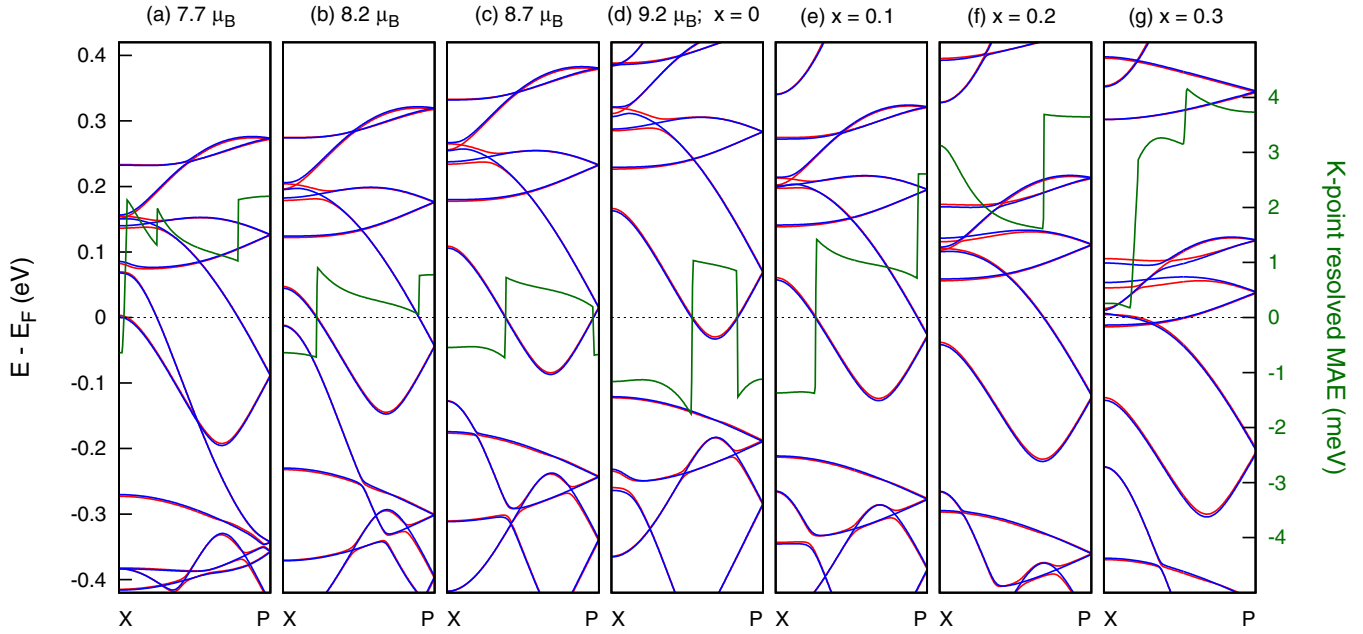
FIG. 13. Band structures calculated in fully relativistic approach for quantization axes 100 (red lines) and 001 (blue lines), together with the MAE contributions of each **k**-point (green line) as obtained by the magnetic force theorem. Panels (d), (c), (b), and (a) depict results for Fe_5SiB_2 with an decreasing fixed spin moment (FSM), in representation of total moment $M_S + M_L$ (μ_B) per formula unit. Panels (d), (e), (f), (g) present increase of Co concentration x in $(Fe_{1-x}Co_x)_5SiB_2$ alloys.
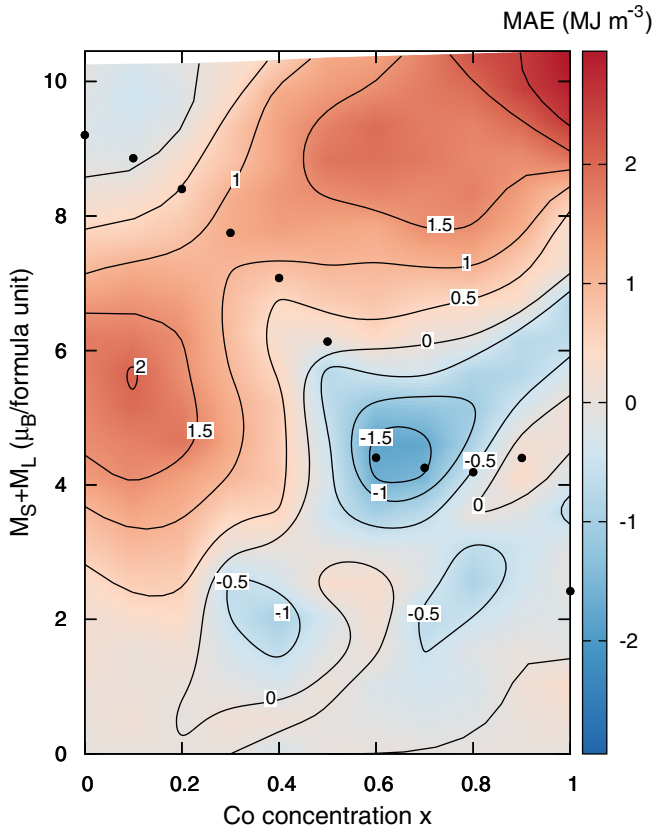

FIG. 14. MAE as a function of x and total magnetic moment $(M_S + M_L)$ for $(Fe_{1-x}Co_x)_5SiB_2$. Disorder was treated by the VCA. $M_S + M_L$ was stabilized with fixed spin moment (FSM) approach. Equilibrium $M_S + M_L$ are denoted by the black dots.

in Fig. 10. Focusing on the uniaxial anisotropy, the highest MAE value along the equilibrium path is reached for the $(Fe_{0.7}Co_{0.3})_5SiB_2$ alloy and is equal to 1.16 MJ/m^3. We note that on the calculated MAE landscape, there is a region with about twice higher values of MAE for $x = 0.1$ and $M_S + M_L$ about 5.8 μ_B/f.u. To approach this region, starting, e.g., from the $(Fe_{0.7}Co_{0.3})_5SiB_2$ composition, both the magnetic moment and the d-electrons number (proportional to x) should be reduced. The desired magnetic moment reduction, from 7.75 to around 5.8 μ_B/f.u., is around 25%. This can be obtained by alloying $(Fe_{0.7}Co_{0.3})_5SiB_2$ with 25% of a suitable nonmagnetic element. The nonmagnetic alloying should at the same time decreases x (which may be understood as the number of d electrons beyond those of Fe) by about 0.2. Such decrease can be obtained by alloying $(Fe_{0.7}Co_{0.3})$ with elements having less of d electrons, i.e., the elements from columns of the periodic table preceding the column with Fe. Among $3d$ elements which fulfill the latter condition are Cr or Mn, but these often carry rather large magnetic moments, therefore they would not fulfill the first condition—reduction of average moment per atom. From $4d$ and $5d$ elements possible candidates are Mo and Tc, or W and Re, respectively.

Similar analysis of MAE landscape as presented above has been previously performed for $(FeCo)_2B$ [11] and led to very similar results. The additional calculations for $(FeCo)_2B$ with W and Re confirmed that these doped systems should exhibit significant increase of MAE. Subsequently conducted synthesis succeeded in producing the $(Fe_{0.675}Co_{0.3}Re_{0.025})_2B$ sample for which the theoretically predicted increase of MAE has been observed [11]. Thus we propose that also for $(Fe_{0.7}Co_{0.3})_5SiB_2$, alloying it with W and Re might help to improve MAE. This is, however,

	Fe$_1$	Fe$_2$	Si	B	Formula
SPRKKR-ASA	1.73	2.63	-0.12	-0.15	9.22
SPRKKR-FP	1.86	2.22	-0.15	-0.16	9.20
FPLO	1.87	2.24	-0.25	-0.25	8.97

outside the scope of the present paper and is left for future investigations.

The VCA yields similar results of MAE as a function of x in (Fe$_{1-x}$Co$_x$)$_5$SiB$_2$ when comparing with (Fe$_{1-x}$Co$_x$)$_2$B [11]. Nevertheless, the VCA may quantitatively overestimate the MAE [11,33,34]. Hence, calculations have also been attempted using the SPRKKR [41,42] method in the atomic sphere approximation (ASA) with the coherent potential approximation (CPA) to treat the alloying. However, it turns out that the SPRKKR-ASA calculations yield magnetic moments in poor agreement with the full potential calculations performed with the FPLO, as illustrated in Table IV. We suspect that the primary reason for this discrepancy is the lack of full-potential effects, since our SPRKKR calculations were done with the same exchange-correlation functional [31] and the ASA might not give an accurate description of magnetic properties in non-close-packed systems [11]. To confirm this suspicion, full potential calculations were also performed for Fe$_5$SiB$_2$ in SPRKKR and as seen in Table IV, the agreement with the FPLO is much better. The failure of the ASA is likely to be related to the empty spaces observed in the structure of this system [16], since it should expected to be a good approximation for close packed structures. The magnetocrystalline anisotropies calculated with the CPA in SPRKKR-ASA (not shown) qualitatively disagree with the FPLO VCA results, but as the MAE is a delicate magnetic property depending sensitively on the electronic structure, we do not consider MAE values obtained in SPRKKR-ASA to be reliable when the magnetic moments are not accurately described. Full potential MAE calculations using CPA are more challenging and beyond the scope of the current paper.

We point out that VCA prediction agrees with the recent experimental results [25] of MAE increase for alloying Fe$_5$SiB$_2$ with Co. McGuire and Parker [25] have observed for (Fe$_{0.8}$Co$_{0.2}$)$_5$SiB$_2$ (Fe$_4$CoSiB$_2$) the increase of anisotropy field accompanied by 20% reduction of magnetic moment, in comparison to the pure Fe$_5$SiB$_2$. Their measurements done on Fe$_5$SiB$_2$ are also in good agreement with our experimental results. For Fe$_5$PB$_2$ Lamichhane *et al.* [26] report experimental values of MAE $= 0.5$ MJ/m^3, and total magnetic moment equal to 8.6 μ_B/f.u. McGuire and Parker [25] calculated in

plane anisotropy with K_1 equal to -0.42 (-0.28) MJ/m^3 with total magnetic moment 9.15 (9.20) μ_B/f.u. for Fe$_5$SiB$_2$, and uniaxial anisotropy with K_1 equal to 0.46 (0.35) MJ/m^3 with total magnetic moment 8.95 (9.15) μ_B/f.u. for Fe$_5$PB$_2$; for comparison the results of our calculations are in parenthesis. The differences between MAE calculated by us and by McGuire and Parker most likely come from the fact that we have used the optimized lattice parameters instead of the experimental ones. The fact that we employed the FPLO and McGuire and Parker used the WIEN2k should not lead to substantial differences [11].

V. SUMMARY AND CONCLUSIONS

We have presented an experimental study of structural and magnetic properties of Fe$_5$SiB$_2$ polycrystalline materials. This study was computationally extended across the whole range of Fe$_5$Si$_{1-x}$P$_x$B$_2$, Fe$_5$P$_{1-x}$S$_x$B$_2$, and (Fe$_{1-x}$Co$_x$)$_5$SiB$_2$ alloys, with an effort to evaluate the magnetocrystalline anisotropy energies. Theoretical study of volume variation and fully relativistic fixed spin moment calculations of stoichiometric Fe$_5$SiB$_2$ evidence a strong inverse dependency between MAE and total magnetic moment, leading to a maximal value of MAE $= 1.78$ MJ/m^3 for $M_S + M_L = 6.15$ μ_B/f.u., while equilibrium magnetic moment is 9.20 μ_B/f.u. Alloying of Fe$_5$SiB$_2$ with Co is suggested to reproduce reduction of magnetic moment. The whole range of (Fe$_{1-x}$Co$_x$)$_5$SiB$_2$ concentrations is calculated and evidence of a MAE maximum is obtained for Co concentration $x = 0.3$, with the value of MAE $= 1.16$ MJ/m^3 and with the magnetic moment 7.75 μ_B/f.u. Thus, (Fe$_{0.7}$Co$_{0.3}$)$_5$SiB$_2$ appears to be a promising candidate for a rare-earth free permanent magnet. Also further increase of MAE of (Fe$_{0.7}$Co$_{0.3}$)$_5$SiB$_2$ is expected by doping with some of $4d$ or $5d$ elements. For Fe$_5$Si$_{1-x}$P$_x$B$_2$ a monotonic trend in MAE has been obtained, suggesting that at low temperatures and below $x \approx 0.8$ the alloys should have in-plane magnetization, while above $x \approx 0.8$ the magnetization should point along the c axis. The overall MAE values are rather low, suggesting that Fe$_5$Si$_{1-x}$P$_x$B$_2$ class of materials can only form soft magnets. On the other hand the hypothetical Fe$_5$P$_{1-x}$S$_x$B$_2$ compositions with sulfur exhibit increased MAE with the highest value of 0.77 MJ/m^3 for Fe$_5$P$_{0.4}$S$_{0.6}$B$_2$ and MAE $= 0.67$ MJ/m^3 for Fe$_5$SB$_2$.

ACKNOWLEDGMENTS

[1] T. Burkert, L. Nordström, O. Eriksson, and O. Heinonen, Phys. Rev. Lett. **93**, 027203 (2004).

[2] G. Andersson, T. Burkert, P. Warnicke, M. Björck, B. Sanyal, C. Chacon, C. Zlotea, L. Nordström, P. Nordblad, and O. Eriksson, Phys. Rev. Lett. **96**, 037205 (2006).

[3] E. K. Delczeg-Czirjak, A. Edström, M. Werwiński, J. Rusz, N. V. Skorodumova, L. Vitos, and O. Eriksson, Phys. Rev. B **89**, 144403 (2014).

[4] L. Reichel, G. Giannopoulos, S. Kauffmann-Weiss, M. Hoffmann, D. Pohl, A. Edström, S. Oswald, D. Niarchos, J.

Rusz, L. Schultz, and S. Fähler, J. Appl. Phys. **116**, 213901 (2014).

[5] L. Reichel, L. Schultz, D. Pohl, S. Oswald, S. Fähler, M. Werwiński, A. Edström, E. K. Delczeg-Czirjak, and J. Rusz, J. Phys. Cond. Matt. **27**, 476002 (2015).

[6] Y. Miura, S. Ozaki, Y. Kuwahara, M. Tsujikawa, K. Abe, and M. Shirai, J. Phys. Cond. Matt. **25**, 106005 (2013).

[7] A. Edström, J. Chico, A. Jakobsson, A. Bergman, and J. Rusz, Phys. Rev. B **90**, 014402 (2014).

[8] T. K. Kim and M. Takahashi, Appl. Phys. Lett. **20**, 492 (1972).

[9] A. Iga, Jpn. J. Appl. Phys. **9**, 415 (1970).

[10] K. D. Belashchenko, L. Ke, M. Däne, L. X. Benedict, T. N. Lamichhane, V. Taufour, A. Jesche, S. L. Bud'ko, P. C. Canfield, and V. P. Antropov, Appl. Phys. Lett. **106**, 062408 (2015).

[11] A. Edström, M. Werwiński, D. Iuşan, J. Rusz, O. Eriksson, K. P. Skokov, I. A. Radulov, S. Ener, M. D. Kuz'min, J. Hong, M. Fries, D. Y. Karpenkov, O. Gutfleisch, P. Toson, and J. Fidler, Phys. Rev. B **92**, 174413 (2015).

[12] M. Däne, S. K. Kim, M. P. Surh, D. Åberg, and L. X. Benedict, J. Phys.: Condens. Matter **27**, 266002 (2015).

[13] H. Fujii, T. Hokabe, T. Kamigaichi, and T. Okamoto, J. Phys. Soc. Jpn. **43**, 41 (1977).

[14] E. K. Delczeg-Czirjak, L. Delczeg, M. P. J. Punkkinen, B. Johansson, O. Eriksson, and L. Vitos, Phys. Rev. B **82**, 085103 (2010).

[15] D. Niarchos, G. Giannopoulos, M. Gjoka, C. Sarafidis, V. Psycharis, J. Rusz, A. Edström, O. Eriksson, P. Toson, J. Fidler, E. Anagnostopoulou, U. Sanyal, F. Ott, L.-M. Lacroix, G. Viau, C. Bran, M. Vazquez, L. Reichel, L. Schultz, and S. Fähler, JOM **67**, 1318 (2015).

[16] B. Aronsson and I. Engström, Acta Chem. Scand. **14**, 1403 (1960).

[17] S. Rundqvist, Acta Chem. Scand. **16**, 1 (1962).

[18] D. A. P. Reis, C. A. Nunes, and A. Capri Neto, Revista Brasileira de Aplicações de Vácuo **26**, 79 (2007).

[19] A. Brauner, C. A. Nunes, A. D. Bortolozo, G. Rodrigues, and A. J. S. Machado, Solid State Commun. **149**, 467 (2009).

[20] M. Fukuma, K. Kawashima, M. Maruyama, and J. Akimitsu, J. Phys. Soc. Jpn. **80**, 024702 (2011).

[21] H. E. Baurecht, H. Boller, and H. Nowotny, Monatshefte für Chemie / Chemical Monthly **102**, 373 (1971).

[22] O. N. Il'nitskaya and Yu. B. Kuz'ma, Sov. Powder Metall. Met. Ceram. **24**, 226 (1985).

[23] T. Ericsson, L. Häggström, and R. Wäppling, Phys. Scr. **17**, 83 (1978).

[24] L. Häggström, R. Wäppling, T. Ericsson, Y. Andersson, and S. Rundqvist, J. Sol. St. Chem. **13**, 84 (1975).

[25] M. A. McGuire and D. S. Parker, J. Appl. Phys. **118**, 163903 (2015).

[26] T. N. Lamichhane, V. Taufour, S. Thimmaiah, D. S. Parker, S. L. Bud'ko, and P. C. Canfield, J. Mag. Magn. Mat. **401**, 525 (2016).

[27] H. M. Rietveld, J. Appl. Cryst. **2**, 65 (1969).

[28] J. Rodriguez-Carvajal, Physica B **192**, 55 (1993).

[29] T. J. B. Holland and S. A. T. Redfern, Mineral. Mag. **61**, 65 (1997).

[30] K. Koepernik and H. Eschrig, Phys. Rev. B **59**, 1743 (1999).

[31] J. P. Perdew, K. Burke, and M. Ernzerhof, Phys. Rev. Lett. **77**, 3865 (1996).

[32] P. Soven, Phys. Rev. B **2**, 4715 (1970).

[33] I. Turek, J. Kudrnovský, and K. Carva, Phys. Rev. B **86**, 174430 (2012).

[34] Y. Kota and A. Sakuma, Appl. Phys. Express **5**, 113002 (2012).

[35] K. Momma and F. Izumi, J. Appl. Crystallogr. **41**, 653 (2008).

[36] C. T. Chen, Y. U. Idzerda, H.-J. Lin, N. V. Smith, G. Meigs, E. Chaban, G. H. Ho, E. Pellegrin, and F. Sette, Phys. Rev. Lett. **75**, 152 (1995).

[37] J. Cedervall, S. Kontos, T. C. Hansen, O. Balmes, F. J. Martinez-Casado, Z. Matej, P. Beran, P. Svedlindh, K. Gunnarsson, and M. Sahlberg, J. Solid State Chem. **235**, 113 (2016).

[38] A. I. Liechtenstein, M. I. Katsnelson, V. P. Antropov, and V. A. Gubanov, J. Mag. Magn. Mat. **67**, 65 (1987).

[39] R. Wu and A. J. Freeman, J. Mag. Magn. Mat. **200**, 498 (1999).

[40] M. Werwiński, J. Kaczkowski, P. Leśniak, W. L. Malinowski, A. Szajek, A. Szczeszak, and S. Lis, Comp. Mat. Sci. **117**, 98 (2016).

[41] H. Ebert, D. Ködderitzsch, and J. Minár, Rep. Prog. Phys. **74**, 096501 (2011).

[42] H. Ebert, The munich spr-kkr package, version 7.2, http://ebert.cup.uni-muenchen.de/SPRKKR.